Supercond. Sci. Technol. **15** (2002) 1454–1466 PII: S0953-2048(02)36390-5

Magnetic fields and currents for two current-carrying parallel coplanar superconducting strips in a perpendicular magnetic field

Ali A Babaei Brojeny[1,2], **Yasunori Mawatari**[3], **M Benkraouda**[4] **and John R Clem**[2,5]

[1] Department of Physics, Isfahan University of Technology, Isfahan 84154, Iran
[2] Department of Physics and Astronomy, Iowa State University, Ames, IA 50011–3160, USA
[3] National Institute of Advanced Industrial Science and Technology, Tsukuba, Ibaraki 305-8568, Japan
[4] Physics Department, PO Box 17551, UAE University, Al-Ain, UAE
[5] Ames Laboratory, Iowa State University, Ames, IA 50011–3160, USA

Received 30 April 2002, in final form 2 September 2002
Published 20 September 2002
Online at stacks.iop.org/SUST/15/1454

Abstract
We present general solutions for the Meissner-state magnetic-field and current-density distributions for a pair of parallel, coplanar superconducting strips carrying arbitrary but subcritical currents in a perpendicular magnetic field. From these solutions we calculate (a) the inductance per unit length when the strips carry equal and opposite currents, (b) flux focusing in an applied field—how much flux per unit length is focused into the slot between the two strips when each strip carries no net current, (c) the current distribution for the zero-flux quantum state when the strips are connected with superconducting links at the ends and (d) the current and field distributions around both strips when only one of the strips carries a net current. The solutions are closely related to those found recently for the magnetic-field and current-density distributions in a thin, bulk-pinning-free, type-II superconducting strip with a geometrical barrier when the strip carries a current in a perpendicular applied field.

1. Introduction

Calculations of the magnetic-field and current-density distributions are of importance in the design of superconducting thin-film devices such as superconducting quantum interference devices (SQUIDs) and passive microwave devices. When superconducting strips in the vortex-free Meissner state carry applied or induced electrical currents, the current density is not uniform across the width of the strip. Because of the strong demagnetizing effects of the strip geometry, the current density is usually higher at the strip edges than in the middle.

In this paper, we present solutions for the distributions of magnetic field and current density for a pair of parallel, coplanar superconducting strips in the Meissner state when the strips carry arbitrary but subcritical currents in the presence of an applied magnetic field. In section 2, we consider the simplest case, that for which the strips are of *equal width* (figure 1(*a*)). General solutions can be obtained by linear superposition of solutions for three separate cases. The first of these, case A, describes the behaviour in a perpendicular applied field when the magnetic flux passes up through the slot between the strips and the current density in the strips flows only in the clockwise direction when viewed from above. These solutions are closely related to those found recently for the magnetic-field and current-density distributions in a thin, bulk-pinning-free, type-II superconducting strip (width $2W$) with a geometrical barrier in a perpendicular applied field [1–4]. In the latter case, no current flows in a vortex-filled region of width $2b$ straddling the centreline, and high

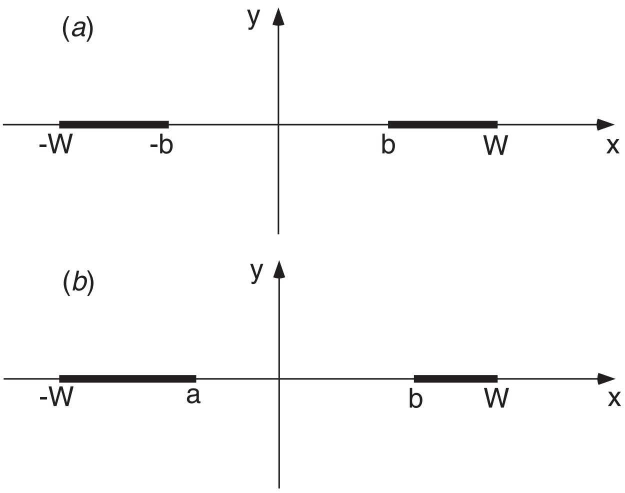

Figure 1. (a) Sketch of geometry considered in section 2: two parallel coplanar superconducting strips of equal width $(W - b)$, separated by a slot of width $2b$, lie in the xz plane. (b) Sketch of geometry considered in section 3: two parallel coplanar superconducting strips of unequal width $(W - b)$ and $(a + W)$, where $a < b$, separated by a slot of width $(b - a)$, lie in the xz plane.

currents flow in vortex-free regions between the edges and the vortex-filled region. The zero-current vortex-filled region corresponds to the slot between the superconducting strips, and the high-current vortex-free regions correspond to the two superconducting strips in the Meissner state considered here.

The second solution, case B, describes the dipole-like behaviour when equal and opposite currents flow in the two strips. The magnetic flux is trapped in the slot between the strips, and the associated current density in the strips flows only in the anticlockwise direction when viewed from above. We calculate the inductance per unit length, which corresponds to that of a coplanar ac transmission line.

The third solution, case C, describes the behaviour when equal currents flow in the same direction in both strips.

By linear superposition of the solutions for cases A, B and C, one may obtain analytic solutions for the magnetic-field and current-density distributions for arbitrary values of the applied magnetic field and arbitrary and possibly unequal currents in the two strips. We confine our attention to currents less than the critical current, such that the strips remain in the Meissner state. We consider the following three cases, which are the ones most likely to be encountered experimentally.

Case D deals with flux focusing when neither strip carries a net current. Solutions obtained by combining cases A and B tell us how much magnetic flux is focused into the slot between the strips. This is analogous to the flux-focusing effect in a washer-type SQUID [5].

Case E deals with the zero-flux quantum state, produced when the two strips are connected at the ends with superconducting links and a perpendicular magnetic field is applied. Solutions obtained by combining A and B describe the induced fields and currents when the net magnetic flux through the slot is zero. The magnetic flux density within the slot is not zero, but its integral vanishes. We calculate the screening efficiency, which we define as the ratio of the magnetic moment of the two strips in the zero-flux quantum state to the magnetic moment of a single strip of width $2W$ in the Meissner state.

Case F deals with a current-carrying line and a zero-net-current spectator line. By combining the solutions for cases B and C, a solution can be found for the magnetic-field and current-density distributions when one of the strips carries a net current but the other strip carries screening currents but no net current.

In section 3, we consider the more difficult case for which the two superconducting strips are of *unequal width* (figure 1(b)). Again we can obtain general solutions for arbitrary applied magnetic fields and arbitrary currents in the two strips by superposition of three independent solutions, which we label as cases A′, B′ and C′. We confine our attention to fields and currents less than their critical values, such that the strips remain in the Meissner state. Case A′ describes the behaviour in a perpendicular applied magnetic field when magnetic flux passes up through the slot between the strips and the current density in the strips flows only in the clockwise direction when viewed from above. However, when the two strips are of unequal width, this occurs together with a net transport current along the strips. The solutions for case A′ are similar to those found recently for the magnetic-field and current-density distributions in a thin, bulk-pinning-free, type-II superconducting strip (width $2W$) with a geometrical barrier when the strip carries a net current in a perpendicular applied field [6]. In the latter case, no current flows in a central vortex-filled region of width $b - a$, and high currents flow in vortex-free regions of width $W - b$ and $a + W$ at the right and left edges of the strip, respectively. The zero-current vortex-filled region corresponds to the slot between the superconducting strips, and the high-current vortex-free regions correspond to the superconducting strips in the Meissner state. Case B′, a dipole-like solution, describes the case when equal and opposite currents flow in the two strips of unequal width, and case C′ describes the case when currents flow in the same direction in both strips.

The solutions for case D′, flux focusing in the presence of an applied field but with no net current flowing in either strip, are obtained by combining the solutions for cases A′, B′ and C′. The solutions for case E′, the zero-flux quantum state produced when the ends of the strips are connected with superconducting links and a magnetic field is applied, are also obtained by combining the solutions for cases A′, B′ and C′. We calculate the screening efficiency, defined as the ratio of the magnetic moment of the two strips in the zero-flux quantum state to the magnetic moment of a single strip of width $2W$ in the Meissner state. The solutions for case F′, for which only one of the strips carries a net current, are obtained by combining the results for cases B′ and C′.

In section 4, we summarize our results.

2. Two strips of equal width

Consider two thin coplanar superconducting strips of equal width in the xz plane in the region $-W < x < W$ (figure 1(a)). They are separated by a slot of width $2b$ $(b < W)$ in the region $-b < x < b$, such that each strip is of width $W - b$. We assume that the strip thickness d obeys $d \ll W - b$ but also that if $d < \lambda$, where λ is the superconducting penetration depth, then $\Lambda \ll W - b$, where $\Lambda = 2\lambda^2/d$ is the 2D screening length [7]. Under such assumptions, magnetic-field penetration into the superconducting strips makes only a negligible perturbation of the magnetic-field distribution calculated from Maxwell's equations using the boundary condition on the strips' surfaces that the normal component of the magnetic flux density vanishes.

When the strips carry current and are subjected to an applied magnetic field, the resulting magnetic field $\mathbf{H}$ is two dimensional; i.e., it is expressible as $\mathbf{H}(x, y) = \hat{x}H_x(x, y) + \hat{y}H_y(x, y)$. Such fields are conveniently described using analytic functions $\tilde{H}(\zeta) \equiv H_y(x, y) + \mathrm{i}H_x(x, y)$ of the complex variable $\zeta \equiv x + \mathrm{i}y$ [3, 8, 9]. Since such analytic functions satisfy the Cauchy–Riemann conditions, they automatically guarantee that both the divergence and the curl of $\mathbf{H}$ vanish.

2.1. Case A—geometrical-barrier-like

The first solutions of interest, which we call case A, describe the behaviour in a perpendicular applied field $\mathbf{H}_a = \hat{y}H_a$ when some magnetic flux passes up through the slot shown in figure 1(*a*) and the current density in the strips flows only in the clockwise direction when viewed from above:

$$\tilde{H}_A(\zeta) = H_a \frac{(\zeta^2 - b^2)^{1/2}}{(\zeta^2 - W^2)^{1/2}}. \qquad (1)$$

Recalling that $\zeta = x + \mathrm{i}y$, we may evaluate the real and the imaginary parts of $\tilde{H}_A$ using the general relations that $(\zeta - a)^{1/2} = (x - a)^{1/2}$ when $x > a$ and $y = 0$, and that $(\zeta - a)^{1/2} = \mathrm{i}(a - x)^{1/2}$ when $x < a$ and $y = \epsilon$, where ϵ is positive infinitesimal. The y component of the magnetic field in the plane of the strip is

$$\begin{aligned} &H_{Ay}(x, 0) \\ &= H_a \frac{|x^2 - b^2|^{1/2}}{|x^2 - W^2|^{1/2}}, \qquad |x| < b \quad \text{or} \quad |x| > W, \qquad (2a) \\ &= 0, \quad \text{otherwise}, \qquad (2b) \end{aligned}$$

and the x component evaluated at $y = \epsilon$ is

$$\begin{aligned} H_{Ax}(x, \epsilon) &= -H_a \frac{x}{|x|} \frac{(x^2 - b^2)^{1/2}}{(W^2 - x^2)^{1/2}}, \\ &\quad b < |x| < W, \qquad (3a) \\ &= 0, \quad \text{otherwise}. \qquad (3b) \end{aligned}$$

Application of Ampere's law and the symmetry that $H_{Ax}(x, \epsilon) = -H_{Ax}(x, -\epsilon)$ yields the current density averaged over the strip thickness, which has only a z component,

$$\begin{aligned} J_{Az}(x) &= \frac{2H_a}{d} \frac{x}{|x|} \frac{(x^2 - b^2)^{1/2}}{(W^2 - x^2)^{1/2}}, \qquad b < |x| < W, \qquad (4a) \\ &= 0, \quad \text{otherwise}. \qquad (4b) \end{aligned}$$

Either by performing a multipole expansion of the Biot–Savart law and using equation (1) or by evaluating the integral, one may show that the dipole moment per unit length [10] in the y direction is

$$m'_{Ay} = -d \int_{-W}^{W} J_{Az}(x) x \, \mathrm{d}x = -\pi H_a (W^2 - b^2). \qquad (5)$$

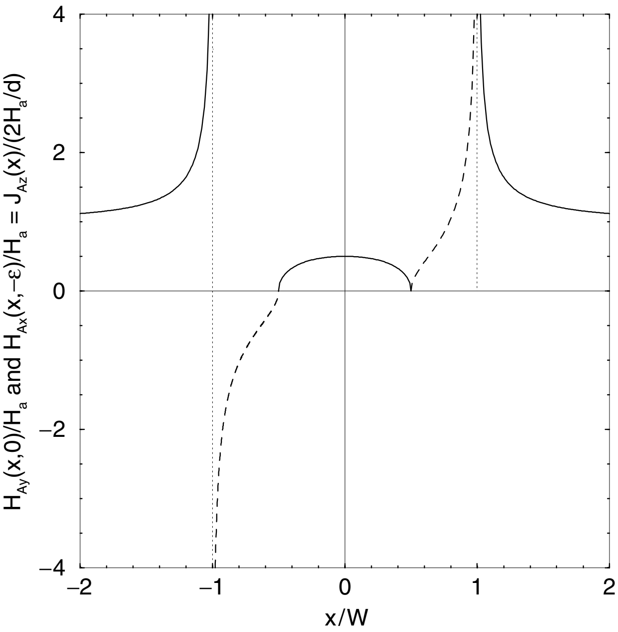

Figure 2. Plots of $H_{Ay}(x, 0)/H_a$ (solid) and $H_{Ax}(x, -\epsilon)/H_a = J_{Az}(x)/(2H_a/d)$ (dashed) versus x/W for the equal-strip-width geometrical-barrier-like case A and $b = 0.5W$.

Figure 2 shows plots of $H_{Ay}(x, 0)$ (solid) and $H_{Ax}(x, -\epsilon)$ or $J_{Az}(x)$ (dashed) for $b = 0.5W$.

Equations (2*a*) and (2*b*) show that the magnetic field has a dome-like distribution within the slot, and equation (4*a*) indicates that the current flows in the clockwise direction when viewed from above. As discussed in section 1, these results correspond to geometrical-barrier solutions found earlier for initial magnetic-flux penetration into a single bulk-pinning-free superconducting strip [1–4].

The magnetic flux per unit length up through the slot Φ'_{Ay} can be evaluated using equations (2*a*), (86), (96) and (97) (see the appendix):

$$\begin{aligned} \Phi'_{Ay} &= \mu_0 \int_{-b}^{b} H_{Ay}(x, 0) \, \mathrm{d}x \\ &= 2\mu_0 H_a W [\mathbf{E}(k) - k'^2 \mathbf{K}(k)], \qquad (6) \end{aligned}$$

where $\mathbf{K}(k)$ and $\mathbf{E}(k)$ are complete elliptic integrals of the first and second kind of modulus $k = b/W$ and complementary modulus $k' = \sqrt{1 - k^2}$. Similarly, the currents I_{AR} and I_{AL} flowing along the z direction in the right ($b < x < W$) and left ($-W < x < -b$) strips may be evaluated using equations (4*a*), (82), (90), (94) and (95):

$$I_{AR} = d \int_{b}^{W} J_{Az}(x) \, \mathrm{d}x = 2H_a W [\mathbf{E}(k') - k^2 \mathbf{K}(k')], \qquad (7)$$

$$I_{AL} = d \int_{-W}^{-b} J_{Az}(x) \, \mathrm{d}x = -I_{AR}, \qquad (8)$$

such that the net current is $I_A = I_{AR} + I_{AL} = 0$.

2.2. Case B—dipole

The second solutions of interest describe the behaviour in the absence of an applied field when some magnetic flux is trapped in the slot and a dipole-like current distribution in the strips flows only in the anticlockwise direction when viewed from above:

$$\tilde{H}_B(\zeta) = -H_0 \frac{W^2}{[(\zeta^2 - b^2)(\zeta^2 - W^2)]^{1/2}}. \tag{9}$$

Evaluating the real and the imaginary parts of $\tilde{H}_B$ as we did for case A, we find that the y component of the magnetic field in the plane of the strip is

$$H_{By}(x,0)$$
$$= -H_0 \frac{W^2}{[(x^2-b^2)(x^2-W^2)]^{1/2}}, \qquad |x| > W, \tag{10a}$$
$$= 0, \quad b < |x| < W, \tag{10b}$$
$$= H_0 \frac{W^2}{[(b^2-x^2)(W^2-x^2)]^{1/2}}, \qquad |x| < b, \tag{10c}$$

and the x component evaluated at $y = \epsilon$ is

$$H_{Bx}(x,\epsilon) = H_0 \frac{x}{|x|} \frac{W^2}{[(x^2-b^2)(W^2-x^2)]^{1/2}},$$
$$b < |x| < W, \tag{11a}$$
$$= 0, \quad \text{otherwise}. \tag{11b}$$

The corresponding current density, which has only a z component, is

$$J_{Bz}(x) = -\frac{2H_0}{d} \frac{x}{|x|} \frac{W^2}{[(x^2-b^2)(W^2-x^2)]^{1/2}},$$
$$b < |x| < W, \tag{12a}$$
$$= 0, \quad \text{otherwise}. \tag{12b}$$

By performing a multipole expansion of the Biot–Savart law and using equation (9), one may show that the dipole moment per unit length [10] in the y direction is

$$m'_{By} = -d \int_{-W}^{W} J_{Bz}(x) x \, dx = 2\pi H_0 W^2. \tag{13}$$

This result also can be obtained by evaluating the integral with the help of equations (12a), (80), (88) and (99). Figure 3 shows plots of $H_{By}(x,0)$ (solid) and $H_{Bx}(x,-\epsilon)$ or $J_{Bz}(x)$ (dashed) for $b = 0.5W$.

The magnetic flux per unit length up through the slot Φ'_{By} can be evaluated using equations (10c), (83) and (96):

$$\Phi'_{By} = \mu_0 \int_{-b}^{b} H_{By}(x,0) \, dx = 2\mu_0 H_0 W \mathbf{K}(k), \tag{14}$$

where $k = b/W$ and $k' = \sqrt{1-k^2}$. The currents I_{BR} and I_{BL} flowing along the z direction in the right ($b < x < W$) and left ($-W < x < -b$) strips may be evaluated using equations (12a), (79), (87) and (94):

$$I_{BR} = d \int_{b}^{W} J_{Bz}(x) \, dx = -2H_0 W \mathbf{K}(k') \tag{15}$$

and

$$I_{BL} = d \int_{-W}^{-b} J_{Bz}(x) \, dx = -I_{BR}. \tag{16}$$

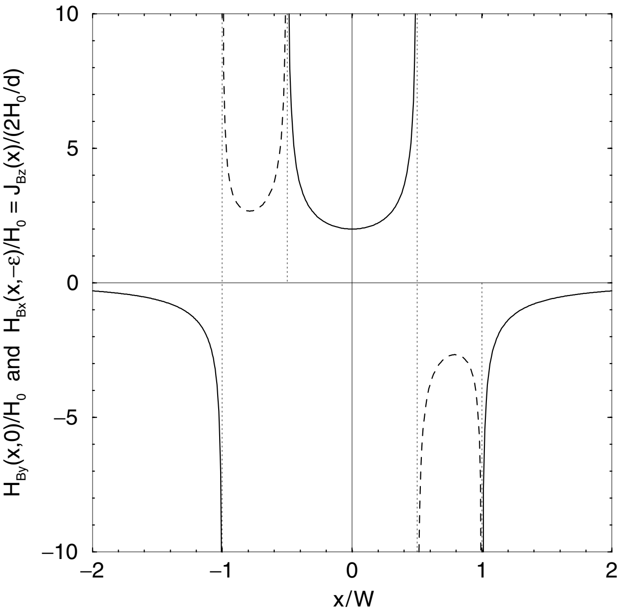

Figure 3. Plots of $H_{By}(x,0)/H_0$ (solid) and $H_{Bx}(x,-\epsilon)/H_0 = J_{Bz}(x)/(2H_0/d)$ (dashed) versus x/W for the equal-strip-width dipole case B and $b = 0.5W$.

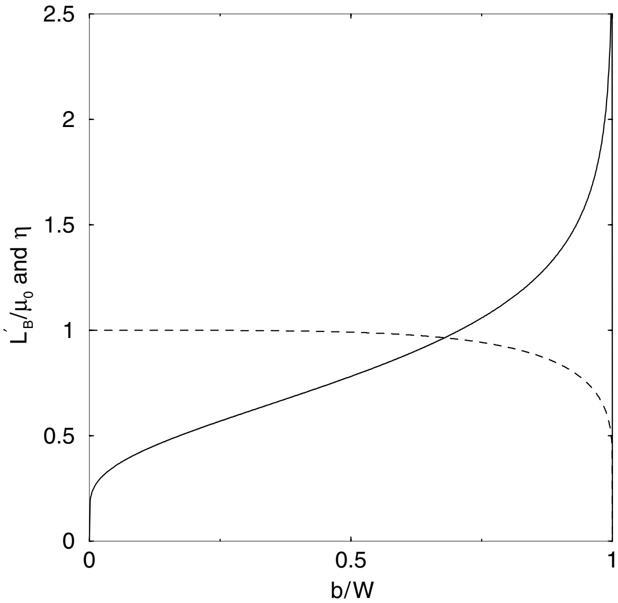

Figure 4. L'_B/μ_0, where L'_B (equation (17)) is the inductance per unit length for the equal-strip-width case B, versus $k = b/W$ (solid curve); and the screening efficiency η (equation (32)) for the zero-flux quantum case E versus $k = b/W$ (dashed).

The inductance per unit length is, therefore,

$$L'_B = \Phi'_{By}/I_{BL} = \mu_0 \mathbf{K}(k)/\mathbf{K}(k'), \tag{17}$$

as found in [11]. This result is the same as that for normal-metal coplanar strips at sufficiently high frequencies that the skin depth is small in comparison with the sample dimensions [12]. The solid curve in figure 4 shows L'_B as a function of $k = b/W$. Note that L'_B diverges logarithmically as $b \to W$.

2.3. Case C—parallel currents

The third solutions of interest describe the behaviour in the absence of an applied field when parallel currents flow in the strips:

$$\tilde{H}_C(\zeta) = \frac{I_t}{2\pi} \frac{\zeta}{[(\zeta^2 - b^2)(\zeta^2 - W^2)]^{1/2}}, \tag{18}$$

where I_t is the total current flowing in the z direction. Evaluating the real and the imaginary parts of $\tilde{H}_C$ as we did for the above cases, we find that the y component of the magnetic field in the plane of the strip is

$$H_{Cy}(x,0) = \frac{I_t}{2\pi} \frac{x}{[(x^2 - b^2)(x^2 - W^2)]^{1/2}}, \quad |x| > W, \tag{19a}$$

$$= 0, \quad b < |x| < W, \tag{19b}$$

$$= -\frac{I_t}{2\pi} \frac{x}{[(b^2 - x^2)(W^2 - x^2)]^{1/2}}, \quad |x| < b, \tag{19c}$$

and the x component evaluated at $y = \epsilon$ is

$$H_{Cx}(x,\epsilon) = -\frac{I_t}{2\pi} \frac{|x|}{[(x^2 - b^2)(W^2 - x^2)]^{1/2}}, \quad b < |x| < W, \tag{20a}$$

$$= 0, \quad \text{otherwise}. \tag{20b}$$

The corresponding current density, which has only a z component, is

$$J_{Cz}(x) = \frac{I_t}{\pi d} \frac{|x|}{[(x^2 - b^2)(W^2 - x^2)]^{1/2}}, \quad b < |x| < W, \tag{21a}$$

$$= 0, \quad \text{otherwise}. \tag{21b}$$

Figure 5 shows plots of $H_{Cy}(x,0)$ (solid) and $H_{Cx}(x,-\epsilon)$ or $J_{Cz}(x)$ (dashed) for $b = 0.5W$.

The magnetic flux per unit length up through the slot Φ'_{Cy}, obtained from equation (19c), is

$$\Phi'_{Cy} = \mu_0 \int_{-b}^{b} H_{Cy}(x,0)\,\mathrm{d}x = 0, \tag{22}$$

because $H_{Cy}(x,0)$ is an odd function of x. The currents I_{CR} and I_{CL} flowing along the z direction in the right ($b < x < W$) and left ($-W < x < -b$) strips may be evaluated using equations (21a), (80), (88) and (99):

$$I_{CR} = d \int_{b}^{W} J_{Cz}(x)\,\mathrm{d}x = I_t/2 \tag{23}$$

and

$$I_{CL} = d \int_{-W}^{-b} J_{Cz}(x)\,\mathrm{d}x = I_t/2. \tag{24}$$

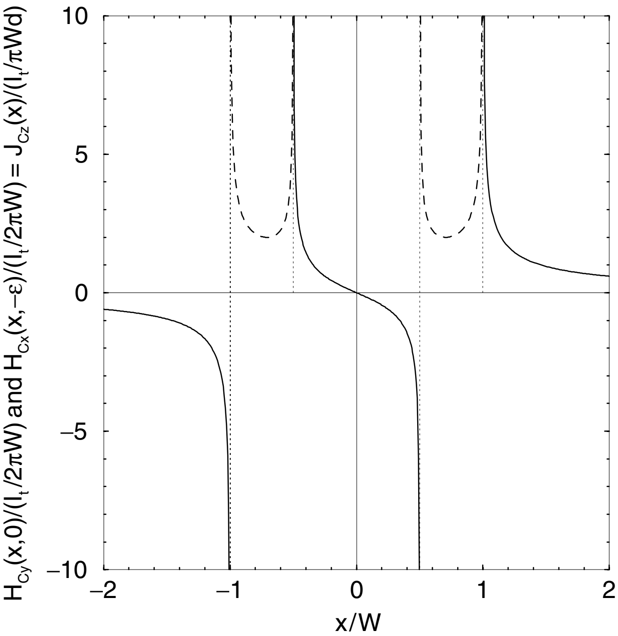

Figure 5. Plots of $H_{Cy}(x,0)/(I_t/2\pi W)$ (solid) and $H_{Cx}(x,-\epsilon)/(I_t/2\pi W) = J_{Cz}(x)/(I_t/\pi W d)$ (dashed) versus x/W for the equal-strip-width parallel-currents case C and $b = 0.5W$.

2.4. Case D—flux focusing

Consider the behaviour when the two strips are subjected to a perpendicular magnetic field H_a but neither strip carries a net current. We wish to calculate how much magnetic flux is focused into the slot. The solutions for case D can be obtained from a linear superposition of the solutions for cases A and B: $\tilde{H}_D(\zeta) = \tilde{H}_A(\zeta) + \tilde{H}_B(\zeta)$, where the constant H_0 in equation (9) is determined by the condition that the current in the right strip is zero ($I_{DR} = I_{AR} + I_{BR} = 0$). From equations (7) and (15) we obtain

$$H_{0D} = [\mathbf{E}(k')/\mathbf{K}(k') - k^2]H_a, \tag{25}$$

where the subscript D labels the value of H_0 for case D. Symmetry guarantees that the current in the left strip also is zero ($I_{DL} = I_{AL} + I_{BL} = 0$). Figure 6 shows plots of $H_{Dy}(x,0)$ (solid) and $H_{Dx}(x,-\epsilon)$ or $J_{Dz}(x)$ (dashed) for $b = 0.5W$.

The magnetic flux per unit length up through the slot is $\Phi'_{Dy} = \Phi'_{Ay} + \Phi'_{By}$, which we obtain from equations (6), (14), (25) and (98). Of the magnetic flux per unit length that is applied to the strip, $2\mu_0 W H_a$, we find that the fraction focused into the slot is

$$\frac{\Phi'_{Dy}}{2\mu_0 W H_a} = \frac{\pi/2}{\mathbf{K}(k')}, \tag{26}$$

where $k = b/W$ and $k' = \sqrt{1-k^2}$. When $k < 1$, this fraction is always less than unity, as shown by the solid curve in figure 7. The ratio of the average magnetic field in the slot to the applied magnetic field is

$$\frac{H_{\text{slot}}}{H_a} = \frac{\Phi'_{Dy}}{2\mu_0 b H_a} = \frac{\pi/2}{k\mathbf{K}(k')}. \tag{27}$$

As $b \to W$, both the focused-flux fraction (equation (26)) and the slot-field ratio (equation (27)) tend to unity. However, as

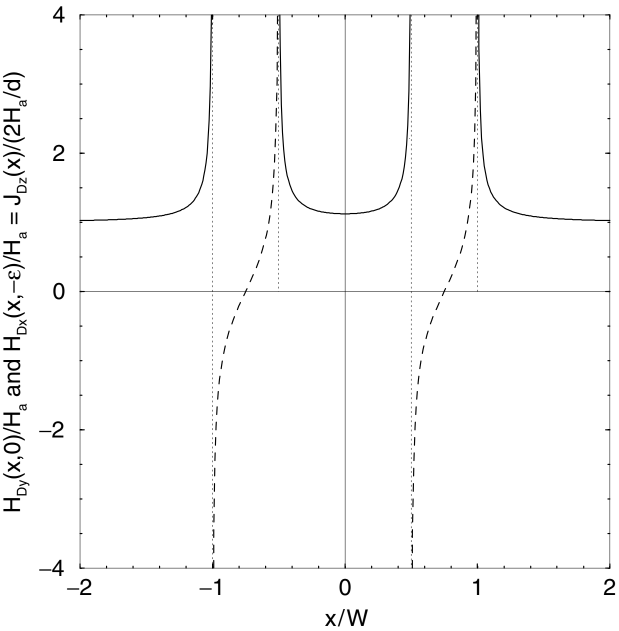

Figure 6. Plots of $H_{Dy}(x, 0)/H_a$ (solid) and $H_{Dx}(x, -\epsilon)/H_a = J_{Dz}(x)/(2H_a/d)$ (dashed) versus x/W for the equal-strip-width flux-focusing case D and $b = 0.5W$.

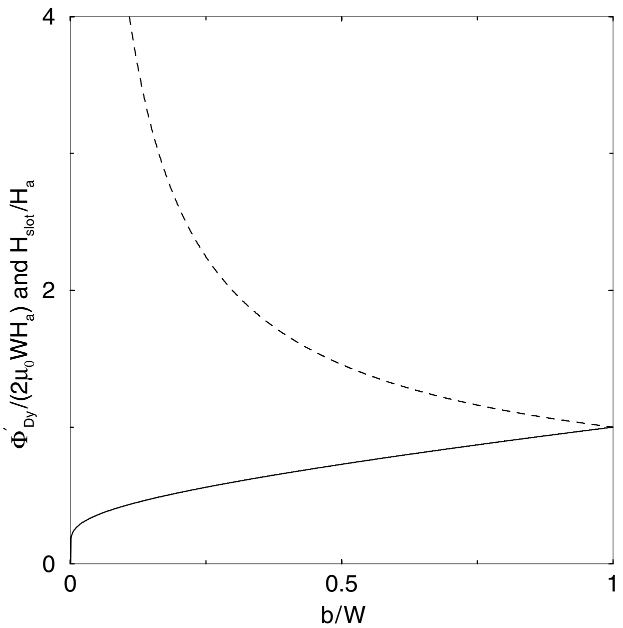

Figure 7. Focused-flux fraction $\Phi'_{Dy}/(2\mu_0 W H_a)$ (equation (26)) (solid) and the slot-field ratio $H_{\rm slot}/H_a$ (equation (27)) (dashed) versus $k = b/W$ for the equal-strip-width flux-focusing case D.

seen in figure 7, as $b \to 0$, the focused-flux fraction (solid) tends to zero, while the slot-field ratio (dashed) diverges. This field enhancement in the slot may have undesired consequences for vortex penetration into dc SQUIDs operated in an ambient magnetic field.

Another way of describing the flux-focusing effect is in terms of the *effective area* of a long slot [5]. Consider a length L_z of the double strip, occupying area $A = 2WL_z$, such that the area of the slot is $A_{\rm slot} = 2bL_z$. The effective area $A_{\rm eff}$

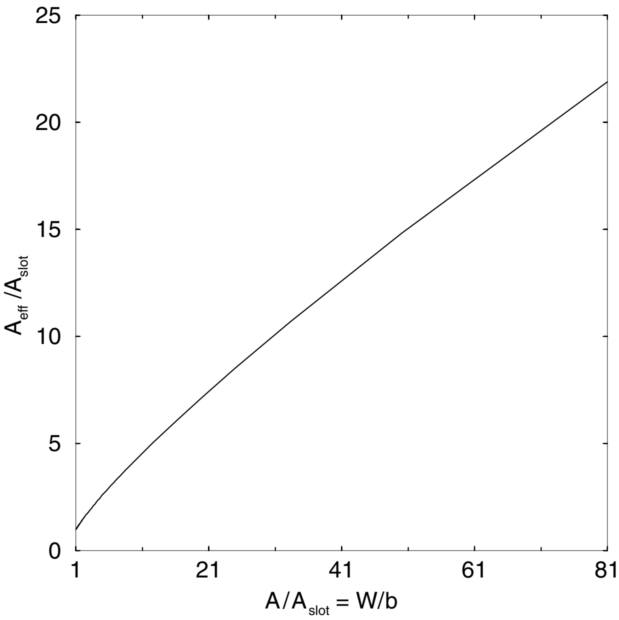

Figure 8. Effective area ratio $A_{\rm eff}/A_{\rm slot}$ (equation (28)) versus $A/A_{\rm slot} = W/b = 1/k$ for the equal-strip-width flux-focusing case D.

of the slot, i.e. the area that would intercept flux $\Phi'_{Dy}L_z$ in a uniform flux density $\mu_0 H_a$, is larger than $A_{\rm slot}$ by the ratio

$$\frac{A_{\rm eff}}{A_{\rm slot}} = \frac{\Phi'_{Dy}L_z/\mu_0 H_a}{2bL_z} = \frac{H_{\rm slot}}{H_a} = \frac{\pi/2}{k\mathbf{K}(k')}. \tag{28}$$

This ratio is shown in figure 8 as a function of $A/A_{\rm slot} = W/b$. For large values of $A/A_{\rm slot}$, $A_{\rm eff}/A_{\rm slot}$ grows approximately linearly with $A/A_{\rm slot}$. This behaviour differs from that of a SQUID loop in the form of a square washer (area A_w) with a square hole (area A_h), for which $A_{\rm eff}/A_h \sim (A_w/A_h)^{1/2}$ [5].

2.5. *Case E—zero-flux quantum state*

Consider next the behaviour when, in the absence of a magnetic field, the two strips are first connected via superconducting links at their ends. A perpendicular magnetic field H_a is now applied in the y direction, but no magnetic flux enters into the strips. When viewed from above, a circulating current flowing in the clockwise direction generates a magnetic field opposing the applied field. The solutions for case E can be obtained from a linear superposition of the solutions for cases A and B: $\tilde{H}_E(\zeta) = \tilde{H}_A(\zeta) + \tilde{H}_B(\zeta)$, where the constant H_0 in equation (9) is now determined by the condition that the net magnetic flux per unit length up through the slot must vanish; i.e., $\Phi'_{Ey} = \Phi'_{Ay} + \Phi'_{By} = 0$. From equations (6) and (14) we obtain

$$H_{0E} = -[\mathbf{E}(k)/\mathbf{K}(k) - k'^2]H_a. \tag{29}$$

The currents in the strips, obtained from $I_{ER} = I_{AR} + I_{BR}$, $I_{EL} = I_{AL} + I_{BL}$, equations (7), (8), (15), (16), (29) and (98), are

$$I_{ER} = -I_{EL} = \pi H_a W/\mathbf{K}(k). \tag{30}$$

Figure 9 shows plots of $H_{Ey}(x, 0)$ (solid) and $H_{Ex}(x, -\epsilon)$ or $J_{Ez}(x)$ (dashed) for $b = 0.5W$.

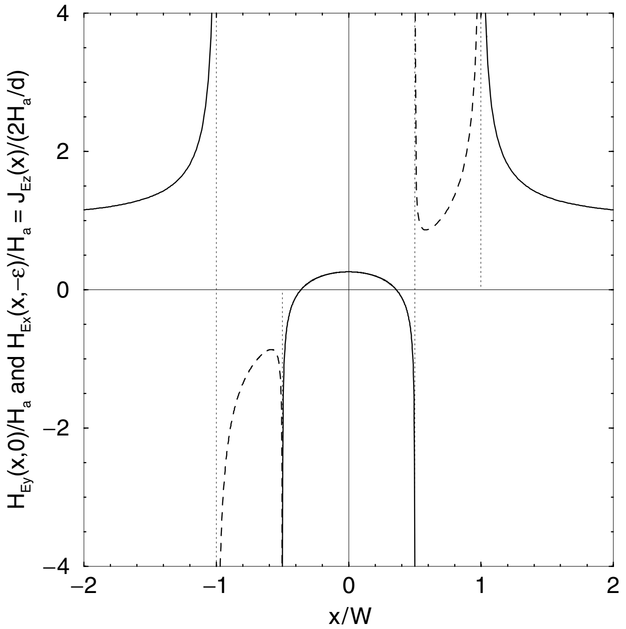

Figure 9. Plots of $H_{Ey}(x, 0)/H_a$ (solid) and $H_{Ex}(x, -\epsilon)/H_a = J_{Ez}(x)/(2H_a/d)$ (dashed) versus x/W for the equal-strip-width zero-flux quantum case E and $b = 0.5W$.

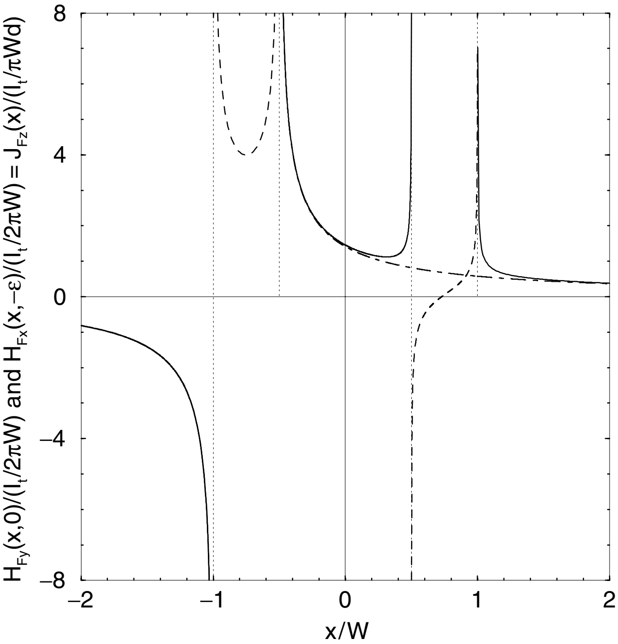

Figure 10. Plots of $H_{Fy}(x, 0)/(I_t/2\pi W)$ (solid) and $H_{Fx}(x, -\epsilon)/(I_t/2\pi W) = J_{Fz}(x)/(I_t/\pi Wd)$ (dashed) versus x/W for the case F (current-carrying strip and a zero-net-current spectator strip of equal width) and $b = 0.5W$. Dot-dashed curves show the same quantities in the absence of the right-hand strip if they differ significantly.

The magnetic moment per unit length of the strip [10] has only a component along the y direction, which is obtained from $J_{Ez} = J_{Az} + J_{Bz}$ and equations (5), (13) and (29):

$$m'_{Ey} = -d \int_{-W}^{W} J_{EZ}(x) x \, \mathrm{d}x = -\pi H_a W^2 [2\mathbf{E}(k)/\mathbf{K}(k) - k'^2]. \tag{31}$$

When $b = 0$, where $k = 0$ and $\mathbf{E}(0) = \mathbf{K}(0) = \pi/2$, the screening is optimum and the magnitude of m'_{Ey} is maximized at $m'_{\max} = -\pi H_a W^2$, the same value as for a solid strip of width $2W$ with no slot. For arbitrary values of $k = b/W < 1$ (recall that $k' = \sqrt{1 - k^2}$), the screening efficiency may be defined as

$$\eta = m'_{Ey}/m'_{\max} = [2\mathbf{E}(k)/\mathbf{K}(k) - k'^2], \tag{32}$$

which is plotted as the dashed curve in figure 4. Note that η remains close to unity for values of k up to around 0.5.

2.6. Case F—only one strip carrying net current

Finally we consider the behaviour when, in the absence of an applied magnetic field, the left strip in figure 1(*a*) carries a transport current I_t but the right strip is simply a passive spectator, carrying no net current. The solutions for this case F can be obtained from a linear superposition of the solutions for cases B and C: $\tilde{H}_F(\zeta) = \tilde{H}_B(\zeta) + \tilde{H}_C(\zeta)$, where the constant H_0 in equation (9) is now determined by the condition that the net current through the right strip must vanish; i.e., $I_{FR} = I_{BR} + I_{CR} = 0$. From equations (15) and (23) we obtain

$$H_{0F} = I_t/4W\mathbf{K}(k'). \tag{33}$$

From equations (16) and (24) we find $I_{FL} = I_{BL} + I_{CL} = I_t$, as expected, and from equations (14), (22) and (33) we obtain the magnetic flux up through the slot, $\Phi'_{Fy} = \Phi'_{By} + \Phi'_{Cy}$:

$$\Phi'_{Fy} = \mu_0 I_t \mathbf{K}(k)/2\mathbf{K}(k'). \tag{34}$$

Figure 10 shows plots of $H_{Fy}(x, 0)$ (solid) and $H_{Fx}(x, -\epsilon)$ or $J_{Fz}(x)$ (dashed) for $b = 0.5W$. The same quantities in the absence of the right spectator strip [10, 13] are shown by dot-dashed curves wherever there are significant differences. For $b = 0.5W$, the differences near the left (current-carrying) strip are insignificant.

3. Two strips of unequal width

We next consider two thin coplanar superconducting strips of unequal width in the xz plane in the region $-W < x < W$, as sketched in figure 1(*b*). The strips are of widths $(W - b)$ and $(a + W)$, where $-W < a < b < W$, and they are separated by a slot of width $(b - a)$. We make the same assumptions on the strip thickness as in section 2, and we again use analytic functions of the complex variable $\zeta \equiv x + \mathrm{i}y$.

3.1. Case A′—geometrical-barrier-like

The solutions for the next case considered, which we call case A′, describe the behaviour in a perpendicular applied field $\mathbf{H}_a = \hat{y} H_a$ when some magnetic flux passes up through the slot and the current density in the strips flows only in the clockwise direction when viewed from above:

$$\tilde{H}_{A'}(\zeta) = H_a \frac{[(\zeta - a)(\zeta - b)]^{1/2}}{(\zeta^2 - W^2)^{1/2}}. \tag{35}$$

Recalling that $\zeta = x + \mathrm{i}y$, we may evaluate the real and the imaginary parts of $\tilde{H}_{A'}$ using the general relations that $(\zeta - a)^{1/2} = (x - a)^{1/2}$ when $x > a$ and $y = 0$, and that $(\zeta - a)^{1/2} = \mathrm{i}(a - x)^{1/2}$ when $x < a$ and $y = \epsilon$, where ϵ is positive infinitesimal. The y component of the magnetic field in the plane of the strip is

$$H_{A'y}(x,0) = H_a \frac{|(x-a)(x-b)|^{1/2}}{|x^2 - W^2|^{1/2}}, \quad a < x < b \quad \text{or} \quad |x| > W, \tag{36a}$$

$$= 0, \quad \text{otherwise}, \tag{36b}$$

and the x component evaluated at $y = \epsilon$ is

$$H_{A'x}(x,\epsilon) = -H_a \frac{[(x-a)(x-b)]^{1/2}}{(W^2 - x^2)^{1/2}}, \qquad b < x < W, \tag{37a}$$

$$= H_a \frac{[(a-x)(b-x)]^{1/2}}{(W^2 - x^2)^{1/2}}, \qquad -W < x < a, \tag{37b}$$

$$= 0, \quad \text{otherwise}. \tag{37c}$$

Application of Ampere's law and the symmetry that $H_{A'x}(x,\epsilon) = -H_{A'x}(x,-\epsilon)$ yields the current density averaged over the strip thickness, which has only a z component,

$$J_{A'z}(x) = \frac{2H_a}{d} \frac{[(x-a)(x-b)]^{1/2}}{(W^2 - x^2)^{1/2}}, \qquad b < x < W, \tag{38a}$$

$$= -\frac{2H_a}{d} \frac{[(a-x)(b-x)]^{1/2}}{(W^2 - x^2)^{1/2}}, \qquad -W < x < a, \tag{38b}$$

$$= 0, \quad \text{otherwise}. \tag{38c}$$

The magnetic moment per unit length, calculated as for case A, is

$$m'_{A'y} = -d \int_{-W}^{W} J_{A'z}(x) x \, \mathrm{d}x = -\pi H_a [W^2 - (b-a)^2/4]. \tag{39}$$

Equations (36a) and (36b) show that the magnetic field has a dome-like distribution within the slot, and equations (38a) and (38b) indicate that currents flow in the clockwise direction when viewed from above. As discussed in section 1, these results correspond to geometrical-barrier solutions found earlier for magnetic-flux penetration into a single bulk-pinning-free superconducting strip carrying a net current in a perpendicular applied magnetic field [6].

The magnetic flux per unit length up through the slot $\Phi'_{A'y}$ can be evaluated in terms of complete elliptic integrals using equations (36a) and (86) (see the appendix):

$$\Phi'_{A'y} = \mu_0 \int_a^b H_{A'y}(x,0) \, \mathrm{d}x = \mu_0 H_a I_8(W,b,a,-W). \tag{40}$$

Similarly, the currents $I_{A'R}$ and $I_{A'L}$ flowing along the z direction in the right ($b < x < W$) and left ($-W < x < a$) strips may be evaluated using equations (38a), (38b), (82) and (90):

$$I_{A'R} = d \int_b^W J_{A'z}(x) \, \mathrm{d}x = 2H_a I_4(W,b,a,-W), \tag{41}$$

$$I_{A'L} = d \int_{-W}^{a} J_{A'z}(x) \, \mathrm{d}x = -2H_a I_{12}(W,b,a,-W). \tag{42}$$

In contrast to case A for equal strip widths, where $I_A = 0$, the total current carried in the z direction for case A′ for unequal strip widths, calculated from equation (35) and Ampere's law, is not zero in general but instead is

$$I_{A'} = I_{A'R} + I_{A'L} = -\pi H_a (a+b), \tag{43}$$

as found in [6]. Alternatively, this can be shown explicitly from equations (41), (42) and (99).

3.2. Case B′—dipole

The next solutions of interest describe the behaviour in the absence of an applied field when some magnetic flux is trapped in the slot and a dipole-like current distribution in the strips flows only in the anticlockwise direction when viewed from above:

$$\tilde{H}_{B'}(\zeta) = -H_0 \frac{W^2}{[(\zeta-a)(\zeta-b)(\zeta^2 - W^2)]^{1/2}}. \tag{44}$$

Evaluating the real and the imaginary parts of $\tilde{H}_{B'}$ as we did for case B, we find that the y component of the magnetic field in the plane of the strip is

$$H_{B'y}(x,0) = -H_0 \frac{W^2}{|(x-a)(x-b)(x^2 - W^2)|^{1/2}}, \qquad |x| > W, \tag{45a}$$

$$= 0, \quad -W < x < a \quad \text{or} \quad b < x < W, \tag{45b}$$

$$= H_0 \frac{W^2}{[(x-a)(b-x)(W^2 - x^2)]^{1/2}}, \qquad a < x < b, \tag{45c}$$

and the x component evaluated at $y = \epsilon$ is

$$H_{B'x}(x,\epsilon) = H_0 \frac{W^2}{[(x-a)(x-b)(W^2 - x^2)]^{1/2}}, \quad b < x < W, \tag{46a}$$

$$= -H_0 \frac{W^2}{[(a-x)(b-x)(W^2 - x^2)]^{1/2}}, \quad -W < x < a, \tag{46b}$$

$$= 0, \quad \text{otherwise}. \tag{46c}$$

The corresponding current density, which has only a z component, is

$$J_{B'z}(x) = -\frac{2H_0}{d} \frac{W^2}{[(x-a)(x-b)(W^2 - x^2)]^{1/2}}, \quad b < x < W, \tag{47a}$$

$$= \frac{2H_0}{d} \frac{W^2}{[(a-x)(b-x)(W^2 - x^2)]^{1/2}}, \quad -W < x < a, \tag{47b}$$

$$= 0, \quad \text{otherwise}. \tag{47c}$$

By performing a multipole expansion of the Biot–Savart law and using equation (44), one may show that the dipole moment per unit length in the y direction is

$$m'_{B'y} = -d \int_{-W}^{W} J_{B'z}(x) x \, \mathrm{d}x = 2\pi H_0 W^2. \qquad (48)$$

This result also can be obtained by evaluating the integral in equation (48) with the help of equations (47*a*), (47*b*), (80), (88) and (99).

The magnetic flux per unit length up through the slot $\Phi'_{B'y}$ can be evaluated using equations (45*c*) and (83):

$$\Phi'_{B'y} = \mu_0 \int_a^b H_{B'y}(x, 0) \, \mathrm{d}x = \mu_0 H_0 W^2 I_5(W, b, a, -W). \qquad (49)$$

The currents $I_{B'R}$ and $I_{B'L}$ flowing along the z direction in the right ($b < x < W$) and left ($-W < x < a$) strips may be evaluated using equations (47*a*), (47*b*), (79) and (87):

$$I_{B'R} = d \int_b^W J_{B'z}(x) \, \mathrm{d}x = -2H_0 W^2 I_1(W, b, a, -W) \qquad (50)$$

and

$$I_{B'L} = d \int_{-W}^{a} J_{Bz}(x) \, \mathrm{d}x = 2H_0 W^2 I_9(W, b, a, -W) = -I_{B'R}, \qquad (51)$$

such that $I_{B'} = I_{B'R} + I_{B'L} = 0$. The inductance per unit length is, therefore,

$$L'_{B'} = \frac{\Phi'_{B'y}}{I_{B'L}} = \frac{\mu_0 I_5(W, b, a, -W)}{2I_1(W, b, a, -W)} = \frac{\mu_0 \mathbf{K}(q')}{2\mathbf{K}(r')}, \qquad (52)$$

where

$$q' = \sqrt{\frac{2W(b-a)}{(W-a)(W+b)}} = \sqrt{1 - r'^2}, \qquad (53)$$

$$r' = \sqrt{\frac{(W-b)(W+a)}{(W-a)(W+b)}} = \sqrt{1 - q'^2}. \qquad (54)$$

That the above expression for $L'_{B'}$ (equation (52)) reduces to that for L'_B (equation (17)) when $a = -b$ can be shown with the help of equations (94) and (96).

3.3. Case C′—parallel currents

The next solutions of interest describe the behaviour in the absence of an applied field when parallel currents flow in the strips:

$$\tilde{H}_{C'}(\zeta) = \frac{I_t}{2\pi} \frac{\zeta}{[(\zeta - a)(\zeta - b)(\zeta^2 - W^2)]^{1/2}}, \qquad (55)$$

where I_t is the total current flowing in the z direction. Evaluating the real and the imaginary parts of $\tilde{H}_{C'}$ as we did for the above cases, we find that the y component of the magnetic field in the plane of the strip is

$$H_{C'y}(x, 0) = \frac{I_t}{2\pi} \frac{x}{[(x-a)(x-b)(x^2 - W^2)]^{1/2}}, \quad |x| > W, \qquad (56a)$$

$$= 0, \quad -W < x < a \quad \text{or} \quad b < x < W, \qquad (56b)$$

$$= -\frac{I_t}{2\pi} \frac{x}{[(x-a)(b-x)(W^2 - x^2)]^{1/2}}, \quad a < x < b, \qquad (56c)$$

and the x component evaluated at $y = \epsilon$ is

$$H_{C'x}(x, \epsilon) = -\frac{I_t}{2\pi} \frac{x}{[(x-a)(x-b)(W^2 - x^2)]^{1/2}}, \quad b < x < W, \qquad (57a)$$

$$= \frac{I_t}{2\pi} \frac{x}{[(a-x)(b-x)(W^2 - x^2)]^{1/2}}, \quad -W < x < a, \qquad (57b)$$

$$= 0, \quad \text{otherwise}. \qquad (57c)$$

The corresponding current density, which has only a z component, is

$$J_{C'z}(x) = \frac{I_t}{\pi d} \frac{x}{[(x-a)(x-b)(W^2 - x^2)]^{1/2}}, \quad b < x < W, \qquad (58a)$$

$$= -\frac{I_t}{\pi d} \frac{x}{[(a-x)(b-x)(W^2 - x^2)]^{1/2}}, \quad -W < x < a, \qquad (58b)$$

$$= 0, \quad \text{otherwise}. \qquad (58c)$$

By performing a multipole expansion of the Biot–Savart law and using equation (55), one may show that the dipole moment per unit length in the y direction is

$$m'_{C'y} = -d \int_{-W}^{W} J_{C'z}(x) x \, \mathrm{d}x = -I_t (a+b)/2. \qquad (59)$$

The magnetic flux per unit length up through the slot $\Phi'_{C'y}$, obtained from equations (56*c*) and (84), is

$$\Phi'_{C'y} = \mu_0 \int_a^b H_{C'y}(x, 0) \, \mathrm{d}x = -(\mu_0 I_t / 2\pi) I_6(W, b, a, -W). \qquad (60)$$

The currents $I_{C'R}$ and $I_{C'L}$ flowing along the z direction in the right ($b < x < W$) and left ($-W < x < a$) strips may be evaluated using equations (58*a*), (58*b*), (80) and (88):

$$I_{C'R} = d \int_b^W J_{C'z}(x) \, \mathrm{d}x = (I_t/\pi) I_2(W, b, a, -W) \qquad (61)$$

and

$$I_{C'L} = d \int_{-W}^{a} J_{C'z}(x) \, \mathrm{d}x = -(I_t/\pi) I_{10}(W, b, a, -W). \qquad (62)$$

That $I_{C'} = I_{C'R} + I_{C'L} = I_t$ can be obtained from equation (55) and Ampere's law. Alternatively, this can be shown explicitly from equations (61), (62) and (99).

3.4. Case D′—flux focusing

We next consider the behaviour when two strips of unequal width are subjected to a perpendicular magnetic field H_a but neither strip carries a net current. We wish to calculate how much magnetic flux is focused into the slot. The solutions for case D′ can be obtained from a linear superposition of the solutions for cases A′, B′ and C′: $\tilde{H}_{D'}(\zeta) = \tilde{H}_{A'}(\zeta) + \tilde{H}_{B'}(\zeta) + \tilde{H}_{C'}(\zeta)$, where the constants H_0 in equation (44) and I_t in equation (55) are determined by the conditions that the net currents in both strips are zero ($I_{D'R} = I_{A'R} + I_{B'R} + I_{C'R} = 0$ and $I_{D'L} = I_{A'L} + I_{B'L} + I_{C'L} = 0$). Since $I_{B'} = 0$ and $I_{C'} = I_t$, the condition that $I_{D'} = I_{A'} + I_{B'} + I_{C'} = 0$ yields, from equation (43),

$$I_{tD'} = -I_{A'} = \pi H_a(a+b), \qquad (63)$$

where the subscript D' labels the value of I_t for case D′. The value of $H_{0D'}$, obtained from the condition that $I_{D'R} = 0$, is

$$H_{0D'} = \frac{2I_4(W,b,a,-W) + (a+b)I_2(W,b,a,-W)}{2W^2 I_1(W,b,a,-W)} H_a \qquad (64a)$$

$$= \frac{(W-a)(W+b)\mathbf{E}(r') + [(W+b)a - (W-a)b]\mathbf{K}(r')}{2W^2\mathbf{K}(r')} H_a, \qquad (64b)$$

where r' is given in equation (54).

The magnetic flux per unit length up through the slot is $\Phi'_{D'y} = \Phi'_{A'y} + \Phi'_{B'y} + \Phi'_{C'y}$, which can be obtained from equations (40), (49), (60), (63), (64b), (77), (78), (83), (84), (86) and (98). Of the magnetic flux per unit length that is applied to the strip, $2\mu_0 W H_a$, the fraction focused into the slot is

$$\frac{\Phi'_{D'y}}{2\mu_0 W H_a} = \frac{\pi\sqrt{(W-a)(W+b)}}{4W\mathbf{K}(r')}. \qquad (65)$$

The ratio of the average magnetic field in the slot to the applied magnetic field is

$$\frac{H'_{\rm slot}}{H_a} = \frac{\Phi'_{D'y}}{\mu_0(b-a)H_a} = \frac{\pi\sqrt{(W-a)(W+b)}}{2(b-a)\mathbf{K}(r')}. \qquad (66)$$

For a long slot of length L_z, the ratio of the effective area $A'_{\rm eff} = \Phi'_{D'y}L_z/\mu_0 H_a$ to the area of the slot $A'_{\rm slot} = (b-a)L_z$ is $A'_{\rm eff}/A'_{\rm slot} = H'_{\rm slot}/H_a$, which can be evaluated using equation (66). For the equal-width case ($a = -b$), equations (65) and (66) reduce to equations (26) and (27), as can be shown with the help of equation (94).

3.5. Case E′—zero-flux quantum state

Consider next the behaviour when, in the absence of a magnetic field, the two strips are first connected via superconducting links at their ends. A perpendicular magnetic field H_a is now applied in the y direction, but no magnetic flux enters into the strips. When viewed from above, a circulating current flowing in the clockwise direction generates a magnetic field opposing the applied field. The solutions for case E′ can be obtained from a linear superposition of the solutions for cases A′, B′ and C′: $\tilde{H}_{E'}(\zeta) = \tilde{H}_{A'}(\zeta) + \tilde{H}_{B'}(\zeta) + \tilde{H}_{C'}(\zeta)$, where the constants H_0 in equation (44) and I_t in equation (55) now are determined by the conditions that (a) the net magnetic flux per unit length up through the slot must vanish ($\Phi'_{E'y} = \Phi'_{A'y} + \Phi'_{B'y} + \Phi'_{C'y} = 0$) and (b) the net current carried by the two strips must vanish ($I_{E'} = I_{A'} + I_{B'} + I_{C'} = 0$). For the same reasons as those leading to equation (63), we find

$$I_{tE'} = \pi H_a(a+b), \qquad (67)$$

where the subscript E' labels the value of I_t for case E′. With the help of equations (40), (49), (60), (83), (84) and (86) we obtain the value of $H_{0E'}$ from the condition that $\Phi'_{E'y} = 0$:

$$H_{0E'} = \frac{(a+b)I_6(W,b,a,-W) - 2I_8(W,b,a,-W)}{2W^2 I_5(W,b,a,-W)} H_a \qquad (68a)$$

$$= -\frac{1}{2}\left[\left(1-\frac{a}{W}\right)\left(1+\frac{b}{W}\right)\frac{\mathbf{E}(q')}{\mathbf{K}(q')} - \left(1+\frac{ab}{W^2}\right)\right] H_a, \qquad (68b)$$

where q' is given in equation (53). That equation (68b) reduces to equation (29) when $a = -b$ can be shown with the help of equations (96) and (97). The currents in the strips, obtained from $I_{E'R} = I_{A'R} + I_{B'R} + I_{C'R}$, $I_{E'L} = I_{A'L} + I_{B'L} + I_{C'L}$ and equations (41), (42), (50), (51), (61), (62), (67), (68b), (79), (80), (82) and (98), are

$$I_{E'R} = -I_{E'L} = \pi H_a\sqrt{(W-a)(W+b)}/\mathbf{K}(q'). \qquad (69)$$

That equation (69) reduces to equation (30) when $a = -b$ can be shown with the help of equation (96).

The magnetic moment per unit length of the strip has only a component along the y direction, which is obtained from $J_{E'z} = J_{A'z} + J_{B'z} + J_{C'z}$ and equations (39), (48), (59), (67) and (68b):

$$m'_{E'y} = -d\int_{-W}^{W} J_{E'z}(x)x\,\mathrm{d}x$$
$$= -\pi H_a[(W-a)(W+b)\mathbf{E}(q')/\mathbf{K}(q') + (a+b)^2/4]. \qquad (70)$$

When $a = b$, where $\mathbf{E}(0) = \mathbf{K}(0) = \pi/2$, the screening is optimum and the magnitude of $m'_{E'y}$ is maximized at $m'_{\max} = -\pi H_a W^2$, the same value as for a solid strip of width $2W$ with no slot. For arbitrary values of a and b the screening efficiency may be defined as

$$\eta' = m'_{E'y}/m'_{\max} = (1-a/W)(1+b/W)\mathbf{E}(q')/\mathbf{K}(q') + (a+b)^2/4W^2, \qquad (71)$$

which has the value unity when $a = b$ but takes on smaller values as a decreases and b increases.

3.6. Case F′—only one strip carrying net current

Finally we consider the behaviour when, in the absence of an applied magnetic field, the left strip in figure 1(b) carries a transport current I_t but the right strip is simply a passive spectator, carrying no net current. The solutions for case F′ can be obtained from a linear superposition of the solutions for cases B′ and C′: $\tilde{H}_{F'}(\zeta) = \tilde{H}_{B'}(\zeta) + \tilde{H}_{C'}(\zeta)$, where the constant H_0 in equation (44) is now determined by the condition that the net current through the right strip must vanish; i.e., $I_{F'R} = I_{B'R} + I_{C'R} = 0$. From equations (50) and (61) we obtain

$$H_{0F'} = (I_t/2\pi W^2) I_2(W, b, a, -W)/I_1(W, b, a, -W) \tag{72a}$$

$$= (I_t/2\pi W^2)\left[a\mathbf{K}(r') + (b-a)\mathbf{\Pi}\left(\frac{W-b}{W-a}, r'\right)\right]\bigg/\mathbf{K}(r'), \tag{72b}$$

where r' is given in equation (54). From equations (51) and (62) we find that $I_{F'L} = I_{B'L} + I_{C'L} = I_t$, as expected. That equation (72*b*) reduces to equation (33) when $a = -b$ can be shown from equation (99).

From equations (49), (60) and (72*b*) we obtain the magnetic flux up through the slot, $\Phi'_{F'y} = \Phi'_{B'y} + \Phi'_{C'y}$:

$$\Phi'_{F'y} = \frac{\mu_0 I_t}{\pi\sqrt{(W-a)(W+b)}}\left[(W-b)\mathbf{\Pi}\left(\frac{b-a}{W-a}, q'\right) - (W-a)\mathbf{K}(q') + (b-a)\mathbf{\Pi}\left(\frac{W-b}{W-a}, r'\right)\mathbf{K}(q')/\mathbf{K}(r')\right], \tag{73}$$

where q' and r' are given in equations (53) and (54). That equation (73) reduces to equation (34) when $a = -b$ can be shown with the help of equations (92), (94) and (96).

4. Summary

In this paper, we presented calculations of the magnetic-field and current-density distributions in the vicinity of two parallel coplanar superconducting strips in the Meissner state. Such calculations assist in understanding the electrodynamic properties of superconducting thin-film devices such as SQUIDs and passive microwave devices. The results apply only when both the strip thickness and the relevant penetration depth (either the London penetration depth λ when $d > \lambda$ or the 2D screening length $\Lambda = 2\lambda^2/d$ when $d < \lambda$) are much smaller than the width of either strip. The results also are valid only if the applied fields and currents are smaller than the critical values that would admit vortices into the strips.

Solutions for arbitrary (but subcritical) applied field and arbitrary (but subcritical) currents in the two strips can be obtained from linear superpositions of the solutions for three simpler cases, which we called cases A, B and C for equal strip widths (figures 2, 3 and 5), and A′, B′ and C′ for unequal strip widths. Cases B and B′ yield the inductance per unit length when the strips carry equal and opposite currents. These solutions also describe the behaviour when magnetic flux is trapped in the slot of a long rectangular superconducting loop.

We studied the flux-focusing effect (cases D and D′), seen in dc SQUIDs, when the two strips are subjected to a perpendicular magnetic field, but neither strip carries a net current. We calculated the focused-flux fraction and the slot-field ratio (i.e., the average field in the slot divided by the applied field). We found that the slot-field ratio, which is a measure of the effective area of the slot, becomes much larger than unity as the slot width decreases to zero.

Next, we examined details of the field and current distributions in the zero-flux quantum state (cases E and E′) produced when the strips are connected via superconducting links at their ends and a magnetic field is then applied. Although the magnetic field in the slot between the two strips is not in general zero, its integral (the magnetic flux up through the slot) is zero.

Finally, we studied the field and current distributions generated when only one of the strips carries a current (cases F and F′). The other strip, a passive spectator, carries induced screening currents and thereby affects the net field distribution.

The magnetic-field distributions for all the above cases should be experimentally observable using recent advances in high-resolution imaging techniques such as magneto-optics [14, 15], scanning SQUID microscopy [16–18], scanning Hall probe microscopy [19, 20] and Lorentz microscopy [21].

Acknowledgments

We thank V G Kogan for stimulating discussions. This work was funded in part by Iowa State University of Science and Technology under contract no W-7405-ENG-82 with the US Department of Energy. The United States Government retains and the publisher, by accepting the paper for publication, acknowledges that the United States Government retains a nonexclusive, paid-up, irrevocable, world-wide license to publish or reproduce the published form of this manuscript, or allow others to do so, for United States Government purposes.

Appendix

The currents in the right and left strips (I_R and I_L) and the flux per unit length (Φ'_y) for all cases considered in this paper were evaluated using the following integrals, obtained partly with the help of [22–24]. The integrals are expressed in terms of complete elliptic integrals of the first kind,

$$\mathbf{K}(k) = \int_0^{\pi/2} \frac{\mathrm{d}\alpha}{\sqrt{1-k^2\sin^2\alpha}} = \int_0^1 \frac{\mathrm{d}x}{\sqrt{(1-x^2)(1-k^2x^2)}}, \tag{74}$$

second kind,

$$\mathbf{E}(k) = \int_0^{\pi/2} \sqrt{1-k^2\sin^2\alpha}\,\mathrm{d}\alpha = \int_0^1 \frac{\sqrt{1-k^2x^2}}{\sqrt{1-x^2}}\,\mathrm{d}x \tag{75}$$

and third kind,

$$\mathbf{\Pi}(n,k) = \int_0^{\pi/2} \frac{\mathrm{d}\alpha}{(1-n\sin^2\alpha)\sqrt{1-k^2\sin^2\alpha}} = \int_0^1 \frac{\mathrm{d}x}{(1-nx^2)\sqrt{(1-x^2)(1-k^2x^2)}}, \tag{76}$$

where k is the *modulus* $k' = \sqrt{1-k^2}$ is the *complementary modulus* and the number n is the *parameter* of the integral of the third kind.

With the convention that $a > b > c > d$ and the definitions

$$q = \sqrt{\frac{(a-d)(b-c)}{(a-c)(b-d)}} = \sqrt{1-r^2}, \tag{77}$$

$$r = \sqrt{\frac{(a-b)(c-d)}{(a-c)(b-d)}} = \sqrt{1-q^2}, \tag{78}$$

the integrals used in this paper are

$$I_1(a,b,c,d) = \int_b^a \frac{\mathrm{d}x}{\sqrt{(a-x)(x-b)(x-c)(x-d)}} = \frac{2}{\sqrt{(a-c)(b-d)}}\mathbf{K}(r), \tag{79}$$

$$I_2(a,b,c,d) = \int_b^a \frac{x\,\mathrm{d}x}{\sqrt{(a-x)(x-b)(x-c)(x-d)}} = \frac{2}{\sqrt{(a-c)(b-d)}}\left[c\mathbf{K}(r) + (b-c)\mathbf{\Pi}\left(\frac{a-b}{a-c}, r\right)\right], \tag{80}$$

$$I_3(a,b,c,d) = \int_b^a \frac{x^2\,\mathrm{d}x}{\sqrt{(a-x)(x-b)(x-c)(x-d)}} = \frac{1}{\sqrt{(a-c)(b-d)}}\Big[(a-c)(b-d)\mathbf{E}(r) - (ab-ac-bc-c^2)\mathbf{K}(r) + (b-c)(a+b+c+d)\mathbf{\Pi}\left(\frac{a-b}{a-c}, r\right)\Big], \tag{81}$$

$$I_4(a,b,c,d) = \int_b^a \sqrt{\frac{(x-b)(x-c)}{(a-x)(x-d)}}\,\mathrm{d}x = \frac{1}{\sqrt{(a-c)(b-d)}}\Big[(a-c)(b-d)\mathbf{E}(r) - (a-c)(b-c)\mathbf{K}(r) + (a-b-c+d)(b-c)\mathbf{\Pi}\left(\frac{a-b}{a-c}, r\right)\Big], \tag{82}$$

$$I_5(a,b,c,d) = \int_c^b \frac{\mathrm{d}x}{\sqrt{(a-x)(b-x)(x-c)(x-d)}} = \frac{2}{\sqrt{(a-c)(b-d)}}\mathbf{K}(q), \tag{83}$$

$$I_6(a,b,c,d) = \int_c^b \frac{x\,\mathrm{d}x}{\sqrt{(a-x)(b-x)(x-c)(x-d)}} = \frac{2}{\sqrt{(a-c)(b-d)}}\left[a\mathbf{K}(q) - (a-b)\mathbf{\Pi}\left(\frac{b-c}{a-c}, q\right)\right], \tag{84}$$

$$I_7(a,b,c,d) = \int_c^b \frac{x^2\,\mathrm{d}x}{\sqrt{(a-x)(b-x)(x-c)(x-d)}} = \frac{1}{\sqrt{(a-c)(b-d)}}\Big[-(a-c)(b-d)\mathbf{E}(q) + (a^2+ab+ac-bc)\mathbf{K}(q) - (a-b)(a+b+c+d)\mathbf{\Pi}\left(\frac{b-c}{a-c}, q\right)\Big], \tag{85}$$

$$I_8(a,b,c,d) = \int_c^b \sqrt{\frac{(b-x)(x-c)}{(a-x)(x-d)}}\,\mathrm{d}x = \frac{1}{\sqrt{(a-c)(b-d)}}\Big[(a-c)(b-d)\mathbf{E}(q) - (a-b)(a-c)\mathbf{K}(q) + (a-b)(a-b-c+d)\mathbf{\Pi}\left(\frac{b-c}{a-c}, q\right)\Big], \tag{86}$$

$$I_9(a,b,c,d) = \int_d^c \frac{\mathrm{d}x}{\sqrt{(a-x)(b-x)(c-x)(x-d)}} = \frac{2}{\sqrt{(a-c)(b-d)}}\mathbf{K}(r), \tag{87}$$

$$I_{10}(a,b,c,d) = \int_d^c \frac{x\,\mathrm{d}x}{\sqrt{(a-x)(b-x)(c-x)(x-d)}} = \frac{2}{\sqrt{(a-c)(b-d)}}\left[b\mathbf{K}(r) - (b-c)\mathbf{\Pi}\left(\frac{c-d}{b-d}, r\right)\right], \tag{88}$$

$$I_{11}(a,b,c,d) = \int_d^c \frac{x^2\,\mathrm{d}x}{\sqrt{(a-x)(b-x)(c-x)(x-d)}} = \frac{1}{\sqrt{(a-c)(b-d)}}\Big[(a-c)(b-d)\mathbf{E}(r) + (b^2+bc+bd-cd)\mathbf{K}(r) - (b-c)(a+b+c+d)\mathbf{\Pi}\left(\frac{c-d}{b-d}, r\right)\Big], \tag{89}$$

$$I_{12}(a,b,c,d) = \int_d^c \sqrt{\frac{(b-x)(c-x)}{(a-x)(x-d)}}\,\mathrm{d}x = \frac{1}{\sqrt{(a-c)(b-d)}}\Big[(a-c)(b-d)\mathbf{E}(r) - (b-c)(b-d)\mathbf{K}(r) - (b-c)(a-b-c+d)\mathbf{\Pi}\left(\frac{c-d}{b-d}, r\right)\Big]. \tag{90}$$

We also have made use of the following identities [22]:

$$(a-d)\mathbf{\Pi}\left(\frac{b-a}{b-d}, r\right) - (b-c)\mathbf{\Pi}\left(\frac{a-b}{a-c}, r\right) = (c-d)\mathbf{K}(r), \tag{91}$$

$$(a-b)\mathbf{\Pi}\left(\frac{b-c}{a-c}, q\right) + (c-d)\mathbf{\Pi}\left(\frac{b-c}{b-d}, q\right) = (a-d)\mathbf{K}(q), \tag{92}$$

$$(a-d)\mathbf{\Pi}\left(\frac{d-c}{a-c}, r\right) - (b-c)\mathbf{\Pi}\left(\frac{c-d}{b-d}, r\right) = (a-b)\mathbf{K}(r), \tag{93}$$

$$\mathbf{K}\left(\frac{1-k'}{1+k'}\right) = \frac{1+k'}{2}\mathbf{K}(k), \tag{94}$$

$$\mathbf{E}\left(\frac{1-k'}{1+k'}\right) = \frac{1}{1+k'}[\mathbf{E}(k) + k'\mathbf{K}(k)], \tag{95}$$

$$\mathbf{K}\left(\frac{2\sqrt{k}}{1+k}\right) = (1+k)\mathbf{K}(k), \tag{96}$$

$$\mathbf{E}\left(\frac{2\sqrt{k}}{1+k}\right) = \frac{1}{1+k}[2\mathbf{E}(k) - k'^2\mathbf{K}(k)], \tag{97}$$

$$\mathbf{E}(k)\mathbf{K}(k') + \mathbf{E}(k')\mathbf{K}(k) - \mathbf{K}(k)\mathbf{K}(k') = \pi/2. \tag{98}$$

Equations (94)–(97) also are valid with k and k' interchanged. We also have made use of the following relation [25]:

$$\mathbf{\Pi}(n,k) + \mathbf{\Pi}(k^2/n,k) - \mathbf{K}(k) = \frac{\pi}{2}\sqrt{\frac{n}{(1-n)(n-k^2)}}, n > 0. \tag{99}$$

References

[1] Indenbom M V, Kronmüller H, Li T W, Kes P H and Menovsky A A 1994 *Physica* C **222** 203
[2] Schuster Th, Indenbom M V, Kuhn H, Brandt E H and Konczykowski M 1994 *Phys. Rev. Lett.* **73** 1424
[3] Zeldov E, Larkin A I, Geshkenbein V B, Konczykowski M, Majer D, Khaykovich B, Vinokur V M and Shtrikman H 1994 *Phys. Rev. Lett.* **73** 1428
[4] Benkraouda M and Clem J R 1996 *Phys. Rev.* B **53** 5716
[5] Ketchen M B, Gallagher W J, Kleinsasser A W, Murphy S and Clem J R 1985 *SQUID '85, Superconducting Quantum Interference Devices and their Applications* ed H D Hahlbohm and H Lübbig (Berlin: de Gruyter) p 865
[6] Benkraouda M and Clem J R 1998 *Phys. Rev.* B **58** 15 103
[7] Pearl J 1964 *Appl. Phys. Lett.* **5** 65
[8] Clem J R, Huebener R P and Gallus D E 1973 *J. Low Temp. Phys.* **12** 449
[9] Mawatari Y and Clem J R 2001 *Phys. Rev. Lett.* **86** 2870
[10] Brandt E H and Indenbom M 1993 *Phys. Rev.* B **48** 12893
[11] Yoshida K, Hossain M S, Kisu T, Enpuku K and Yamafuji K 1992 *Japan. J. Appl. Phys.* **31** 3844
[12] Gupta K C, Garg R, Bahl I and Bhartia P 1996 *Microstrip Lines and Slotlines* 2nd edn (Boston, MA: Artech House Publishers) pp 85, 400
[13] Zeldov E, Clem J R, McElfresh M and Darwin M 1994 *Phys. Rev.* B **49** 9802
[14] Johansen T H, Basiljevich M, Shantsev D V, Goa P E, Galperin Y M, Kang W N, Kim H J, Choi E M, Kim M-S and Lee S I 2001 *Supercond. Sci. Technol.* **14** 726
[15] Goa P E, Hauglin H, Baziljevich M, Il'yashenko E, Gammel P L and Johansen T H 2001 *Supercond. Sci. Technol.* **14** 729
[16] Tsuei C C and Kirtley J R 2000 *Phys. Rev. Lett.* **85** 182
[17] Tafuri F and Kirtley J R 2000 *Phys. Rev.* B **62** 13934
[18] Wynn J C, Bonn D A, Gardner B W, Lin Y-J, Liang R, Hardy W N, Kirtley J R and Moler K A 2001 *Phys. Rev. Lett.* **87** 197002
[19] Oral A, Bending S J and Henini M 1996 *Appl. Phys. Lett.* **69** 1324
[20] Grigorenko A N, Bending S J and Gregory J K 2001 *Appl. Phys. Lett.* **78** 1586
[21] Tonomura A, Kasai H, Kamimura O, Matsuda T, Harada K, Nakayama Y, Shimoyama J, Kishio K, Hanaguri T, Kitazawa K, Sasase M and Okayasu S 2001 *Nature* **412** 620
[22] Gradshteyn I S and Ryzhik I M 2000 *Table of Integrals, Series, and Products* 6th edn, ed A Jeffrey and D Zwillinger (San Diego: Academic)
[23] *Handbook of Mathematical Functions* 1967 ed M Abramowitz and I A Stegun (Washington: National Bureau of Standards)
[24] *Mathematica, Version 4.1* 2000 Wolfram Research, Inc., Champaign, IL
[25] Selfridge R B and Maxfield J E 1958 *A Table of the Incomplete Elliptic Integrals of the Third Kind* (New York: Dover)